Characterization of Membrane Translocation by Anthrax Protective Antigen†

Jørgen Wesche,‡,§,|| Jennifer L. Elliott,||,⊥ Pål Ø. Falnes,‡,§,|| Sjur Olsnes,‡,§ and R. John Collier*,⊥

Department of Microbiology and Molecular Genetics, Harvard Medical School, 200 Longwood Avenue, Boston, Massachusetts 02115, and Department of Biochemistry, Institute for Cancer Research at the Norwegian Radium Hospital, Montebello, 0310 Oslo, Norway

Received June 17, 1998; Revised Manuscript Received September 3, 1998

ABSTRACT: Solving the crystallographic structure of the ring-shaped heptamer formed by protective antigen (PA), the B moiety of anthrax toxin, has focused attention on understanding how this oligomer mediates membrane translocation of the toxin's A moieties. We have developed an assay for translocation in which radiolabeled ligands are bound to proteolytically activated PA (PA_{63}) at the surface of CHO or L6 cells, and translocation across the plasma membrane is induced by lowering the pH. The cells are then treated with Pronase E to degrade residual surface-bound material, and protected ligands are quantified after fractionation by SDS−PAGE. Translocation was most efficient (35%−50%) with LF_N, the N-terminal PA binding domain of the anthrax lethal factor (LF). Intact LF, edema factor (EF), or fusion proteins containing LF_N fused to certain heterologous proteins [the diphtheria toxin A chain (DTA) or dihydrofolate reductase (DHFR)] were less efficiently translocated (15%−20%); and LF_N fusions to several other proteins were not translocated at all. LF_N with different N-terminal residues was found to be degraded according to the N-end rule by the proteasome, and translocation of LF_N fused to a mutant form of DHFR with a low affinity for methotrexate (MTX) protected cells from the effects of MTX. Both results are consistent with a cytosolic location of protected proteins. Evidence that a protein must unfold to be translocated was obtained in experiments showing that (i) translocation of LF_NDTA was blocked by introduction of an artificial disulfide into the DTA moiety, and (ii) translocation of LF_NDHFR and LF_NDTA was blocked by their ligands (MTX and adenine, respectively). These results demonstrate that the acid-induced translocation by anthrax toxin closely resembles that of diphtheria toxin, despite the fact that these two toxins are unrelated and form pores by different mechanisms.

Although many bacterial toxins act by modifying cytosolic substrates within mammalian cells, it is not known in detail for any toxin how the enzymic moiety crosses a membrane. Most intracellularly acting toxins are bipartite proteins, consisting of separable enzymic (A) and delivery (B) moieties. In general the B moiety facilitates attachment of the toxin to the cell surface by binding to cell surface receptors, and in some toxins B also forms aqueous pores in membranes. The actual mechanism by which the translocation occurs remains speculative.

Anthrax toxin (AT[1]) is a term used to describe a collection of three proteins secreted by *Bacillus anthracis*, the causative agent of anthrax. The three proteins are the following: protective antigen (PA; 83 kDa), edema factor (EF; 89 kDa), and lethal factor (LF; 83 kDa). Whereas any of the three proteins alone is nontoxic, injection of EF + PA (a combination termed "edema toxin") causes edema in experimental animals, and injection of LF + PA ("lethal toxin") causes death (*1, 2*). EF and LF are alternative A moieties, and PA serves as the common B moiety for delivery of these proteins into cells (*1, 3*). EF is a calmodulin-dependent adenylate cyclase (*4*), and recent work has shown that LF is a zinc metalloprotease that can cleave MAP-kinase-kinase (*5, 6, 7*). Lethal toxin elicits overproduction of certain lymphokines by macrophages, causing lethal systemic shock (*8*).

Figure 1 shows a current model of the toxin self-assembly and entry pathways involved in AT action on cells. PA binds to an as yet unidentified receptor at the cell surface and is proteolytically activated by furin or a furin-like protease (*9*), yielding N-terminal 20 kDa and C-terminal 63 kDa fragments (PA_{20} and PA_{63}, respectively). Dissociation of PA_{20} allows PA_{63}, which remains bound to the receptor, to oligomerize, forming a ring-shaped heptamer (*10*). The heptamer, which we term the prepore, binds EF or LF competitively, and the complex is internalized by receptor-mediated endocytosis and trafficked to an acidic compartment within the cell (*11*). There, the low pH induces the prepore to insert into the membrane, allowing EF/LF to cross the membrane and enter

† This work was supported by USPHS Grant AI22021 (to R.J.C.); and by Novo Nordisk Foundation, The Norwegian Research Council, Blix Fund, Rachel and Otto Kr. Bruun's legat, and The Jahre Foundation (to S.O.).

* To whom correspondence should be addressed. Tel: 617-432-1930. Fax: 617-432-0115. E-mail: jcollier@hms.harvard.edu.

‡ Institute for Cancer Research at the Norwegian Radium Hospital.

§ Fellow of the Norwegian Cancer Society.

|| These authors contributed equally to this work.

⊥ Harvard Medical School.

[1] Abbreviations: AT, anthrax toxin; DHFR, dihydrofolate reductase; DT, diphtheria toxin; DTA, the catalytic subunit of DT; EF, edema factor; LF, lethal factor; LF_N, N-terminal 255 residues of LF; MES, 4-morpholineethanesulfonic acid; MTX, methotrexate; nPA, trypsin-nicked protective antigen; PA, protective antigen; PA_{20}, N-terminal 20 kDa fragment of PA; PA_{63}, C-terminal 63 kDa fragment of PA; PAGE, polyacrylamide gel electrophoresis; PBS, phosphate-buffered saline.

10.1021/bi981436i CCC: $15.00
Published on Web 10/26/1998

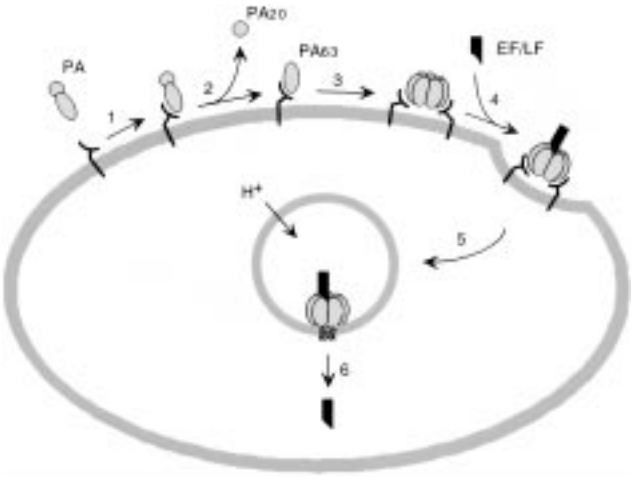

FIGURE 1: Model of anthrax toxin entry into cells: 1, binding of PA to its receptor; 2, proteolytic activation of PA and dissociation of PA_{20}; 3, self-association of monomeric PA_{63} to form the heptameric prepore; 4, binding of EF/LF to the prepore; 5, endocytosis of the receptor/PA_{63}/ligand complex; 6, pH-dependent insertion of PA_{63} and translocation of the ligand.

the cytosol (*12*, *13*). It has been proposed that the pore formed by PA_{63} serves as a conduit for passage of the partially or completely unfolded A moieties across the membrane, but direct evidence for this is lacking.

In many respects the entry mechanism of AT closely resembles that of diphtheria toxin (DT). Both toxins are trafficked to an acidic intracellular compartment (*14*, *15*); in both, the translocation is pH-dependent (*16*) and is blocked by lysosomotropic agents (*14*, *15*); and in both, the B moiety is capable of forming ion-conductive pores in cells and artificial lipid bilayers under acidic conditions (*17*, *18*). AT and DT are structurally unrelated, however, and their insertion into membranes is mediated by entirely different structural motifs. In DT, pore formation is a property of the α-helical T (transmembrane) domain (*17*). This domain contains a buried hydrophobic helical hairpin, which inserts and forms pores upon contact of the domain with negatively charged bilayers under low-pH conditions (*19*). The molecularity of the DT pore remains uncertain, but there is evidence suggesting that it is monomeric (*20*). In contrast, pore formation by AT is mediated by the heptameric PA_{63} prepore (*10*), and recent evidence indicates that the prepore inserts by forming a 14-stranded transmembrane β barrel like that seen in the heptameric *Staphylococcus aureus* α hemolysin pore (*21*, *22*).

Availability of the crystallographic structures of native PA and the PA_{63} heptamer (*23*) has raised the prospect of understanding the AT translocation process in detail. To document more clearly that PA_{63} ligands are in fact translocated to the cytosol and to examine various factors that affect the AT translocation process, we have developed a protease protection assay for acid-triggered translocation by AT across the plasma membrane. Here we describe this assay and its application, together with activity based assays, to quantify AT translocation and to examine factors that affect the efficiency of the process.

EXPERIMENTAL PROCEDURES

Materials, Media, and Buffers. Translation-grade [^{35}S] methionine and [^{3}H] leucine were obtained from Amersham or NEN-Dupont. Methotrexate was from Lederle Arzneimittel (Germany). Pronase E (Protease Type XIV from *Streptomyces griseus*), PMSF, and *N*-ethylmaleimide were purchased from Sigma. HEPES medium consists of the following: bicarbonate- and serum-free Eagle's minimal essential medium (for L6) or Ham's F-12 (for CHOK1), buffered with HEPES to pH 7.4. Dialysis buffer consists of the following: 140 mM NaCl, 20 mM HEPES, and 2 mM $CaCl_2$, adjusted to pH 7.0 with NaOH. Lysis buffer consists of the following: 0.1 M NaCl, 20 mM NaH_2PO_4, 10 mM EDTA, 1% Triton X-100, 1 mM PMSF, and 1 mM NEM, pH 7.4. PBS consists of the following: 140 mM NaCl and 10 mM NaH_2PO_4, pH 7.4. MES/gluconate buffer consists of the following: 140 mM NaCl, 5 mM sodium gluconate, and 20 mM MES, adjusted with Tris to pH 4.8 or 7.0.

Plasmid Construction. The *Escherichia coli* strain DH5α was used in the cloning procedures. To form pB-LF_N-Stop, the fragment encoding residues 1−255 of LF was cloned into pBSN-1 by PCR using pET15b-LF_N (*24*) as a template. The forward primer (CAGTGCCATGGCGGGCGGTCATGGT) was used to introduce a 5′ *Nco*I site, and the reverse primer (CAGTGTCTAGACTAGGATAGATTTATTTCTTG) was used to introduce a stop codon after residue 255 and a 3′ *Xba*I site. The fragment was cloned into pBSN-1 between the *Nco*I and *Xba*I sites. The same strategy was applied to form pB-LF_N-Fus except that instead of a stop codon, a linker containing an *Apa*I site was introduced before the *Xba*I site at the 3′ end of LF_N, using the following reverse primer: CAGTGTCTAGATTGGGCCCCGGATAGATTTATTTCTTG. Fusion proteins were made by introducing a 5′ *Apa*I site and a 3′ *Asp*718 site by PCR in the following coding sequences: aFGF (primers: CAGTAGGGGCCCAAATGGCTAATTACAAGAAG and TCAGTGGGTACCTCAATCAGAAGAGACTGGCAG), bFGF (primers: CAGTAGGGGCCCAAATGGCAGCCGGGAGCATC and TCAGTGGGTACCTCAGCTCTTAGCAGACATTG), DHFR (primers: CAGTAGGGGCCCAAATGGTTCGACCATTGAAC and TCAGTGGGTACCTTAGTCTTTCTTCTCGTAG), DHFR-L22R (primers: CAGTAGGGGCCCAAATGGTTCGACCATTGAACandTCAGTGGGTACCTTAGTCTTTCTTCTCGTAG), CNTF (primers: CAGTAGGGGCCCAAATGGCTTTCGCAGAGCandTCAGTGGGTACCCTACATCTGCTTATCTTTG), Tat (primers: CAGTAGGGGCCCAAATGGAACCAGTCGACCCTAG and TCAGTGGGTACCCTATTCCTTAGGACCTGTC), Tetanus toxin light chain (primers: CAGTAGGGGCCCAAATGCCAATAACCATAAATAAT and TCAGTGGGTACCTTATGCAGTTCTATTATATAAATT), and Botulinum toxin E light chain (primers: CAGTAGGGGCCCAAATGCCAACAATTAATAGTTTTAAT and TCAGTGGGTACCTTATTTCCTTATGCCTTTTACAGAAAC). The fragments were cloned into pB-LF_N-Fus between the *Apa*I and *Asp*718 sites. To form pB-DHFR-LF_N, *Nco*I sites were introduced at the 5′ and 3′ ends of DHFR by PCR (primers: CAGTGCCATGGTTCGACCATTGAAC and GCCCGCCATGGCGTCTTTCTTCTCGTAGAC). The fragment was cloned into the *Nco*I site in pB-LF_N-Stop.

Pre-Arg-FLAG-LF_N was constructed by PCR using pB-LF_N-Fus as a template, the following forward primer: CAGTGCCATGGCACATATCGAGGGAAGGCGATACAAGGACGACGATGACAAGCTCGCGGGCGGTCATGGTGATGTAGGT,

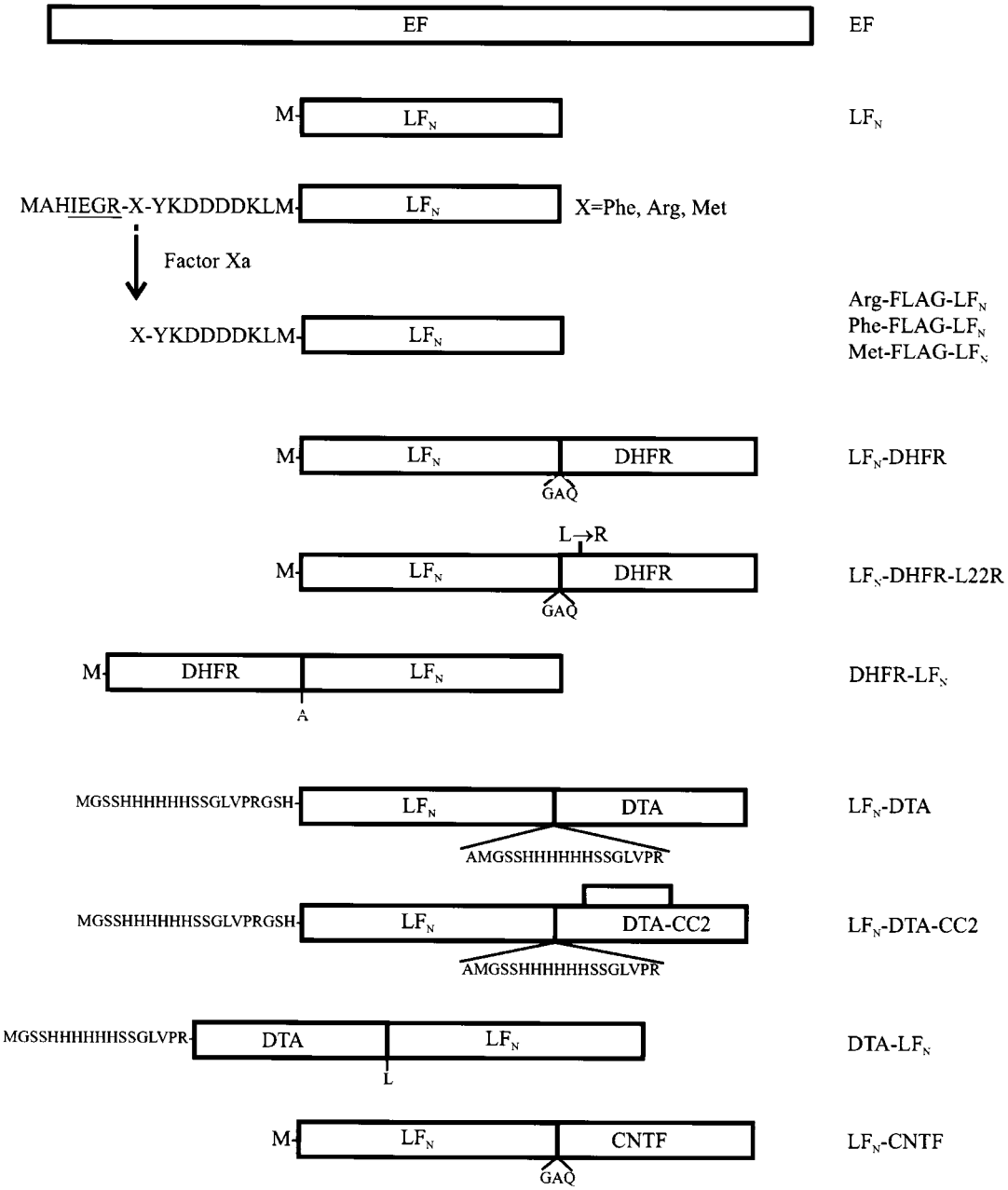

FIGURE 2: Schematic presentation of fusion proteins. In the case of the X-FLAG-LF$_N$ mutants, a precursor containing a factor Xa recognition sequence (underlined) was cleaved with factor Xa, thereby generating X-FLAG-LF$_N$.

and the same reverse primer used in the construction of pB-LF$_N$-Fus. The PCR product was digested with *Nco*I and *Bgl*II and cloned between the *Nco*I and *Bgl*II sites of pB-LF$_N$-Stop. Pre-Met-FLAG-LF$_N$ and pre-Phe-FLAG-LF$_N$ were constructed by similar approaches, but the underlined CGA triplet of the forward primer shown above had been substituted by ATG and TTT, respectively.

LF$_N$DTA-CC2, containing the mutations N58C and S146C, was constructed by PCR using the construct encoding DTA-CC2 (*25*) as template, the forward primer GCAGAAGCAC-CACGTGGCGCTGATGATGTTGTTGAT and the reverse primer AAGCTTGGATCCTCATTAACGATTTCCTGCAG-AGGCTTGAGC, which also alters the natural cysteine at DTA position 186 to a serine. The companion construct, LF$_N$DTA-CS2, was made the same way but using as a template the construct encoding DTA-CS2 (*25*), to result in the single mutation N58C. PCR products were cleaved with the restriction endonucleases *Pml*I and *Bam*HI (New England Biolabs) and introduced into the pET15b LF$_N$DTA construct (*10*) by fragment exchange.

All constructs were verified by dideoxy sequencing, and schematic representations of the constructs used are in Figure 2.

Cell Cultures. CHO-K1 and L6 cells were obtained from the American Type Culture Collection. L6 (rat myoblast) cells were propagated in Dulbecco's modified essential medium (DMEM) supplemented with 5% FCS. CHO-K1 (hamster ovary) cells were propagated in HAM's F12 supplemented with 10% calf serum, 500 units/mL penicillin G, and 500 units/mL streptomycin sulfate (Gibco BRL). Cells were maintained at 5% CO_2 in a humidified atmosphere. Cells were seeded into 12- or 24-well Costar (Cambridge,

MA) microtiter plates 16−18 h preceding the experiments.

In Vitro Transcription and Translation. Plasmid DNA was linearized downstream of the encoding gene and transcribed with T3 RNA polymerase. The mRNA was precipitated with ethanol and dissolved in H_2O containing 10 mM DTT and 0.1 unit/μL RNasin. The translation was performed for 1 h at 30 °C in micrococcal nuclease treated rabbit reticulocyte lysate (Promega, Madison, WI). Radioactive proteins were made with lysates containing 1 μM [^{35}S] methionine and the other 19 amino acids (25 μM). Labeled methionine was replaced by 25 μM unlabeled methionine when making nonradioactive proteins. Alternatively, plasmid DNA containing the gene for the protein of interest was prepared by midiprep (Qiagen) and followed by inclusion in the TNT Coupled Rabbit Reticulocyte Lysate System with T7 polymerase, as per manufacturer instruction (Promega). The amount of protein in the nonlabeled lysates was estimated as earlier described (*26*) by translating in parallel a small aliquot of the lysate in the presence of 5 μM [^{35}S] methionine. Labeled proteins were dialyzed overnight at 4 °C to remove unreacted [^{35}S] methionine.

SDS−PAGE. Polyacrylamide gel electrophoresis in the presence of sodium dodecyl sulfate was carried out in 12.5% gels as described by Laemmli (*27*). After electrophoresis the gel was fixed for 30 min in 27% methanol/4% acetic acid and then incubated for 30 min in 1 M sodium salicylate/2% glycerol, pH 5.8. Kodak XAR-5 film was exposed to the dried gel at −80 °C. Gels examined by phosphorimager were not treated with the enhancing solution.

Cell Binding and Translocation Assay. CHO-K1 or L6 cells were incubated with trypsin-nicked PA (*24*) (2×10^{-8} M) for 2 h at 4 °C. The unbound PA was removed by washing twice with PBS at 4 °C. Radiolabeled protein was added, and the cells were further incubated for 2 h at 4 °C. The cells were then washed three times with PBS and exposed to MES/gluconate buffer (37 °C) at pH 4.8 or 7.0 for 30 s to 2 min. The cells were then either lysed for 10 min in lysis buffer on ice or treated with protease type XIV (Pronase E, 4 mg/mL) for 8 min at 37 °C. The cells, which detach from the plastic during treatment with protease, were collected in Eppendorf tubes and centrifuged. The pelleted cells were washed with Hepes medium containing 1 mM PMSF and 1 mM NEM and lysed for 10 min in lysis buffer on ice. The nuclei were removed from the lysed cells by centrifugation. Proteins were precipitated with 5% TCA for 30 min on ice and pelleted by centrifugation. The pellet was washed twice with ethyl ether and subjected to SDS−PAGE under reducing conditions followed by phosphorimaging or autoradiography.

In Vitro Degradation of LF_N Mutants. [^{35}S] methionine-labeled LF_N mutants obtained by in vitro translation were cleaved with 1 μg of factor Xa/100 μL of translocation mixture for 2 h at 25 °C. Freshly thawed reticulocyte lysate (12 μL) was added to 3 μL of the [^{35}S] methionine-labeled LF_N mutants, and the mixture was incubated at 37 °C (*28*). Bestatin (40 μg/mL) was present since this compound potentiates the effect of dipeptide inhibitors (*29*). At different time points, aliquots were removed and analyzed by SDS−PAGE as previously described (*28*).

Purification of PA and LF_NDTA Proteins. Proteins were overexpressed and purified from the *E. coli* expression strain BL21 (DE3) bearing the appropriate plasmid construct (PA: pET22B-PA (*22*); LF_NDTA proteins, as above). Overnight cultures were added 1:100 to Luria broth containing 50 μg/mL ampicillin. Cultures were grown with shaking at 37 °C until an OD_{600} of 1.0 was reached. IPTG was added to 0.5 mM, and cultures were incubated with shaking at 37 °C for LF_NDTA proteins, 30 °C for PA, for an additional 2 or 4 h, respectively. LF_NDTA-containing cells were harvested by centrifugation and lysed by treatment with lysozyme (100 μg/mL) at 30 °C for 30 min followed by brief sonication (*30*). Lysates were cleared by centrifugation and loaded to a charged Ni^{2+} column (Novagen). Eluted proteins were desalted and further purified by fast-protein liquid chromatography, using the anion-exchange Mono Q column (Pharmacia). LF_NDTA proteins were treated with Cu^{2+}-phenanthroline and dialyzed extensively versus 20 mM Tris, pH 8.0, to ensure efficient formation of disulfide bonds (*31*).

Periplasmic extracts were prepared from PA-containing cells by suspension in 20% sucrose, 30 mM Tris, pH 8.0, followed by centrifugation and resuspension of the cellular pellet in 5 mM $MgSO_4$. Extracts were concentrated and desalted by an Amicon hollow fiber ultrafiltration device. PA was purified from periplasmic extracts by anion exchange using the Q-Sepharose column (Pharmacia), followed by Mono Q purification (Pharmacia).

Protein Synthesis Inhibition Assay. This assay was performed essentially as previously described (*24*). Briefly, CHO cells in 24-well plates were incubated with 2×10^{-8} M nPA and varying concentrations of either WT LF_NDTA, LF_NDTA-CC2, or LF_NDTA-CS2, from 10^{-10} to 10^{-15} M, for 24 h. Proteins were reduced, where specified, with 1 mM DTT prior to incubation with cells. Cells were washed and incubated in leucine-free medium containing 1 μCi/mL [^{3}H] leucine for 1 h. Cells were washed, and total cellular protein was precipitated with 5% TCA. Tritium-incorporated protein was measured by scintillation counting (LKB Wallac) and reported as a percentage of radioactivity incorporated by cells untreated with toxin.

Measurement of Methotrexate Toxicity. L6 cells growing as monolayers in 24-well plates were incubated with increasing amounts of methotrexate in DMEM. In the cases where AT fusion proteins were added, the cells were preincubated with the proteins for 3 h. After 2 days, the medium was changed and the same amount of methotrexate and proteins as before the change were added. The cells were further incubated for 2 days. The last 20 min of the incubation time [^{3}H] leucine was added. The cells were then washed twice with 5% TCA and dissolved in 0.1 M KOH. The amount of incorporated [^{3}H] leucine was estimated by liquid scintillation counting of the lysed material.

RESULTS

Pronase Protection Assay for Translocation. When cells with surface-bound anthrax edema toxin are exposed to low pH, one observes an elevation in the concentration of cAMP within cells, suggesting that some fraction of the bound EF is translocated across the plasma membrane (*11, 32*). This is only indirect evidence for translocation, however, and does not permit quantification of translocated EF. We therefore devised a direct assay for the translocation, involving protection of radiolabeled PA ligands from digestion by Pronase E.

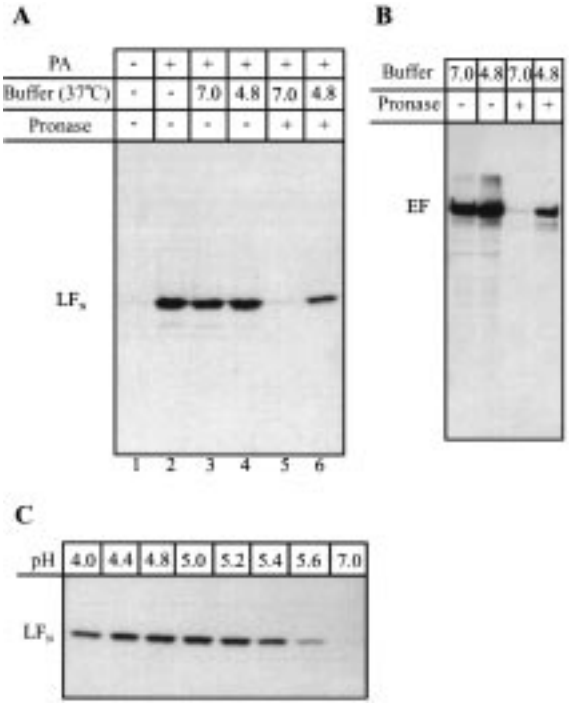

FIGURE 3: Pronase protection assay for translocation. (A) L6 cells were incubated with (lanes 2−6) or without (lane 1) nPA for 2 h at 4 °C, washed, and incubated further with radiolabeled LF_N for 2 h at 4 °C. The cells were then in some cases lysed directly (lanes 1 and 2). In other cases they were briefly incubated at 37 °C with a buffer of acidic (lanes 4 and 6) or neutral pH (lane 3 and 5), and in some cases subsequently treated with Pronase (lanes 5 and 6). Finally, the cells were lysed, the nuclei were removed, and the proteins were TCA-precipitated from the cell lysate and analyzed by SDS−PAGE followed by fluorography. (B) CHO-K1 cells were incubated with nPA and EF and treated as in (A). (C) L6 cells were treated as in (A), but the cells were exposed to buffers with the indicated pH during the brief incubation at 37 °C.

Trypsin-nicked PA was bound to CHO-K1 or L6 cells, the cells were washed, and a PA-ligand protein that had been radiolabeled with [^{35}S] methionine was bound to the cell-associated PA. These steps were performed at 4 °C to inhibit endocytosis. The cells were then incubated at 37 °C for 30 s with acidic (pH 4.8) or neutral (pH 7.0) buffer and subsequently treated with Pronase E. Finally, the cells were lysed, the nuclei were sedimented, and the TCA-precipitable fraction of the supernatant was analyzed by SDS−PAGE.

As one example of a PA ligand, we used LF_N, the 255-residue N-terminal domain of LF. Figure 3A shows that radiolabeled LF_N bound to the cells at 4 °C in the presence but not in the absence of PA, as expected. When cells with bound LF_N were incubated at 37 °C and then treated with Pronase E to digest surface-bound material, a protected band was visible when the incubation had been performed at pH 4.8, but not at pH 7.0. By quantifying the bands from Figure 3A by autoradiography, we estimated that 35%−50% of cell-bound LF_N was translocated. Translocation of LF_N was measured as a function of pH and found to be maximal at pH 5.2 and below (Figure 3C); little translocation was observed at pH 5.6 or higher. In other experiments, we found that 15%−20% of the surface-bound EF (Figure 3B) was translocated. A similar efficiency was observed for LF_N-DTA, a fusion protein of LF_N with the enzymic A chain of DT. Translocation did not occur when the low-pH pulse took place at 4 °C (data not shown).

N-End Rule Mediated Degradation as a Translocation Marker. To obtain further evidence that the protected material was in fact translocated to the cytosol, we prepared mutants of LF_N that could be degraded at different rates by the N-end rule pathway, which involves proteasomes and is believed to occur in the cytosol (for review, see ref 33). According to the N-end rule, the identity of the N-terminal amino acid can strongly influence the intracellular half-life of a protein. Prototypic destabilizing residues are bulky and hydrophobic (i.e., Phe, Trp, Tyr, Leu) or charged amino acids. N-end rule-mediated degradation in vitro can be inhibited by a dipeptide with an N-terminal residue similar to that of the substrate protein (*29*, *34*).

Falnes and Olsnes have studied the N-end rule-mediated degradation of DT mutants (*28*). When a short peptide, the FLAG epitope (*35*), containing an N-terminal Asp residue was fused to the N-terminus of the DT A-fragment, the resulting protein was unstable upon translocation to the cytosol. Furthermore, when this N-terminal Asp was replaced by other amino acids, a panel of mutants with a wide range of intracellular stabilities was generated. The FLAG peptide, with either destabilizing residues (Arg, Phe) or a stabilizing residue (Met) at the N-terminus, was fused to the N-terminus of LF_N, and the constructs were expressed in a rabbit reticulocyte lysate system. Since proteins expressed in a reticulocyte lysate have an N-terminal Met residue, each mutant was produced from a precursor protein containing a factor Xa cleavage site, and the desired N-terminal amino acid was exposed through cleavage with factor Xa.

To test whether the mutants with destabilizing amino acids at the N-terminus could be degraded by the N-end rule pathway, we first studied the stability of the LF_N mutants in vitro in a reticulocyte lysate. We also tested whether the degradation could be inhibited by dipeptides with N-terminal amino acids similar to those of the substrate proteins. Radiolabeled LF_N mutants were cleaved with factor Xa and incubated for different time periods in the lysate. The two mutants with destabilizing amino acids (Arg-FLAG-LF_N and Phe-FLAG-LF_N) were degraded in the lysate, while the mutant with an N-terminal Met (Met-FLAG-LF_N) was not (Figure 4A). The dipeptide with a positively charged amino acid at the N-terminus, His-Ala, inhibited the degradation of Arg-FLAG-LF_N, whereas the dipeptide Trp-Ala, with an N-terminal bulky, hydrophobic amino acid, inhibited the degradation of Phe-FLAG-LF_N (Figure 4A).

We then tested whether the mutants with destabilizing amino acids at the N-terminus could be degraded by the N-end rule pathway in living cells. Radiolabeled LF_N mutants were bound to L6 cells saturated with nPA, and the cells were treated with buffer at pH 4.8 to induce translocation of the mutants. LF_N with a destabilizing N-terminal amino acid (Arg-FLAG-LF_N, Phe-FLAG-LF_N) was rapidly degraded after translocation into the cells, while LF_N with N-terminal Met was stable (Figure 4B). These results indicate that the LF_N mutants are specifically recognized and degraded by the N-end rule pathway both in vitro and in living cells.

The proteasome, a large cytosolic complex, is involved in the degradation of proteins by the N-end rule pathway. Degradation by the proteasome can be inhibited by lacta-

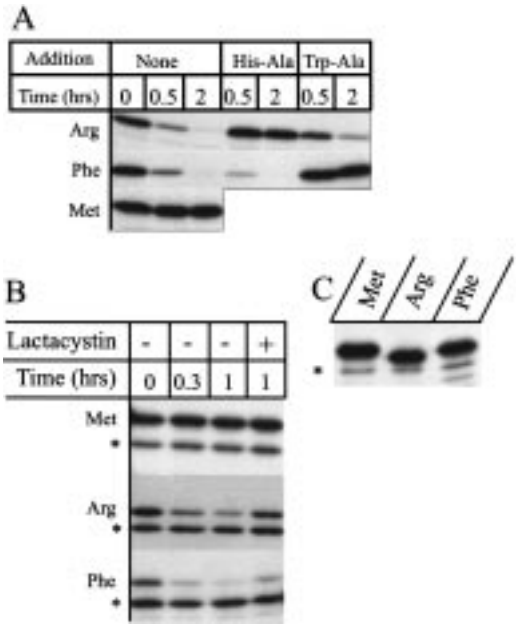

FIGURE 4: N-end rule-mediated degradation of X-FLAG-LF_N. (A) In vitro degradation of LF_N mutants in reticulocyte lysates. After expression in a reticulocyte lysate, precursor proteins were cleaved with factor Xa to generate the corresponding X-FLAG-LF_N proteins (X = Arg, Phe, Met) (see Figure 2). A sample of translation mixture was mixed with an excess of freshly thawed reticulocyte lysate and incubated at 37 °C. At the indicated time points aliquots were removed and analyzed by SDS−PAGE and fluorography. Similar experiments were carried out in the presence of the dipeptides His-Ala and Trp-Ala (10 mM) as indicated. (B) In vivo degradation of X-FLAG-LF_N in L6 cells. Trypsin-nicked PA and [^{35}S] methionine-labeled LF_N mutants were bound to cells at 4 °C as in Figure 3A. The cells were incubated for 2 min at 37 °C in MES/gluconate buffer (pH 4.8) to induce X-FLAG-LF_N translocation, followed by incubation in growth medium for various time periods at 37 °C. Finally, the cells were lysed, and the TCA-precipitable material was analyzed by SDS−PAGE and fluorography. Similar experiments were performed in the presence of the proteasome inhibitor lactacystin. In these cases, the cells were pretreated for 1 h at 37 °C with 20 μM lactacystin, which was also present during the binding of the LF_N mutants to the cells, and during the incubation in growth medium at 37 °C following the low-pH treatment. (C) Binding of X-FLAG-LF_N to cells. L6 cells were incubated with nPA for 2 h at 4 °C, washed, and further incubated with radiolabeled X-FLAG-LF_N mutants for 2 h at 4 °C. The cells were then lysed in lysis buffer and analyzed by SDS−PAGE and fluorography. The asterisk indicates a downstream initiation product that in all cases has an N-terminal methionine.

cystin (*36*). As seen in Figure 4B, the degradation of Arg-FLAG-LF_N and Phe-FLAG-LF_N was inhibited by lactacystin, indicating that the unstable proteins are degraded by the proteasome and supporting the idea that the Pronase-protected material actually has reached the cytosol. The data in Figure 4C demonstrate the ability of the in vitro made protein to bind to cells. In addition to the main translation product, a slightly more rapidly migrating band was observed (indicated by an asterisk). This represents a downstream initiation product which will in all cases have an N-terminal methionine. This protein, which lacks the FLAG peptide, appears to be more easily translocated than the larger protein (compare panels B and C). This protein was stable under all conditions, thus representing an internal control in the experiments in panel B.

Translocation of LF_N Fusion Proteins. Evidence has been presented that when certain peptides and proteins are fused

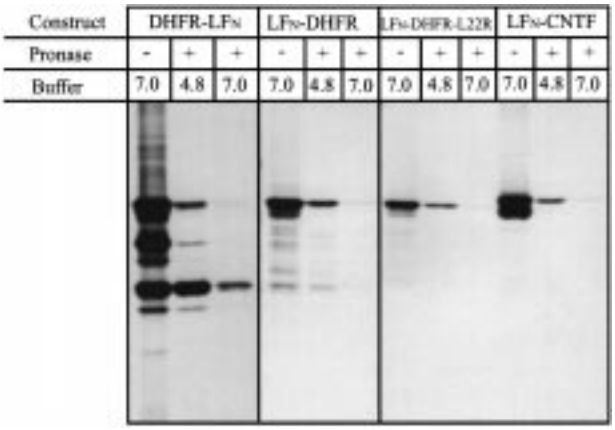

FIGURE 5: Translocation of LF_N fusion proteins. The experiments were performed as in Figure 3A. Trypsin-nicked PA and radiolabeled ligand were bound to cells at 4 °C, and then exposed to pH 4.8 or 7.0. The cells were treated with Pronase where indicated and analyzed by SDS−PAGE and fluorography. The left panel was exposed for a longer period than the others to visualize the translocated fusion proteins.

to LF_N, the resulting heterologous proteins are translocated to the cytosol in a PA-dependent fashion (*24*, *37*−*39*). We used the protease protection assay to test the translocation of a panel of LF_N fusion proteins (see Figure 2).

Dihydrofolate reductase (DHFR), a cytosolic protein, was fused N- or C-terminally to LF_N to form DHFR-LF_N or LF_N-DHFR, and the fusion proteins were bound to the cells in the presence of PA. A Pronase-protected band was visible with both constructs when the cells were treated with buffer at low pH, implying that the fusion proteins were translocated to the cytosol. The translocation was most efficient when DHFR was fused to the C-terminal end of LF_N (Figure 5). Similar experiments were performed with DTA fused to either terminus of LF_N (DTA-LF_N and LF_N-DTA) (*24*), and in this case as well, more material was protected from Pronase when DTA was fused to the C-terminus of LF_N (data not shown). These experiments suggest that the translocation of LF_N fusion proteins is more efficient when the proteins are fused to the C-terminus of LF_N than to its N-terminus, a conclusion consistent with the findings of Arora and co-workers (*38*).

A fusion of ciliary neurotrophic factor to the C-terminus of LF_N (LF_N-CNTF) was also translocated to the cytosol (Figure 5), whereas fusions of several other proteins were not translocated: acidic fibroblast growth factor, tetanus toxin light chain, basic fibroblast growth factor, HIV Tat protein, and botulinum toxin E light chain (data not shown).

A Mutant DHFR Inhibits the Cytotoxicity of Methotrexate in L6 Cells. Dihydrofolate reductase (DHFR) catalyzes the reduction of dihydrofolate to tetrahydrofolate and is a key enzyme in the synthesis of DNA. Methotrexate (MTX), a folate analogue, binds to DHFR and inhibits its enzymatic activity. MTX is therefore used as a cytostatic agent to kill dividing cells.

We constructed a fusion between LF_N and a mutant DHFR that has very low affinity for MTX (LF_N-DHFR-L22R) (*40*). As shown in Figure 5, the fusion protein LF_N-DHFR translocated to the cytosol, and this was also the case for LF_N-DHFR-L22R. We reasoned that this mutant DHFR fusion protein, after translocation into cells, could complement the endogenous DHFR inhibited by MTX.

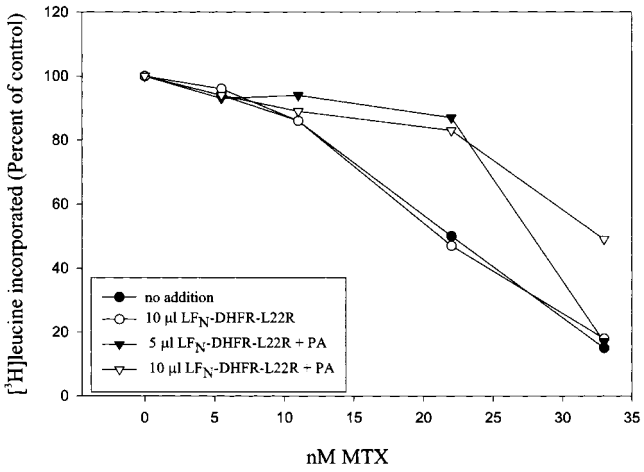

FIGURE 6: Inhibition of MTX cytotoxicity by LF_N-DHFR-L22R. L6 cells were incubated for 4 days with increasing concentrations of MTX (filled circles). In parallel experiments, the cells were incubated with MTX and 10 μL of dialyzed in vitro translated LF_N-DHFR-L22R (open circles), 10 μL of LF_N-DHFR-L22R + nPA (open triangles), and 5 μL of LF_N-DHFR-L22R + nPA (filled triangles). Ten microliters of in vitro translated protein corresponds to ~5 ng of the fusion protein. The last 20 min of the incubation time, [^{3}H]leucine was present, and the incorporated [^{3}H]leucine was estimated by liquid scintillation counting. The data shown are representative of three experiments with similar results.

L6 cells were incubated with various amounts of MTX (0−33 nM). Radiolabeled leucine was added 20 min before termination of the incubation, and the incorporated radioactivity was measured. A dose-dependent decrease in the incorporated radioactivity demonstrated the toxicity of MTX (Figure 6). In parallel experiments, we added LF_N-DHFR-L22R together with PA. In this case, the toxicity of MTX was inhibited. When the fusion protein was added in the absence of PA, there was little or no inhibition of the toxicity (Figure 6). The experiment was repeated three times with similar results. The results imply that LF_N-DHFR-L22R is translocated to the cytosol of L6 cells, where its enzymatic activity can complement the reduced activity of the endogenous DHFR.

Unfolding of a Protein is Required for its Translocation. Unfolding has been shown to be a prerequisite for the translocation of DT to the cytosol. In one study, the introduction of internal disulfide bonds in DTA inhibited translocation of the toxin (*25*); in another, translocation of a fusion between DTA and DHFR was inhibited by methotrexate (MTX), which stabilizes the conformation of DHFR and prevents unfolding (*41*).

To determine if unfolding is also required for AT translocation, we first examined the effect of liganding on LF_N-DHFR translocation. As shown in Figure 7B, translocation of LF_N-DHFR and DHFR−LF_N was inhibited by MTX, whereas the ligand did not interfere with binding of the fusion proteins to the cells (Figure 7A). With the mutant DHFR fusion protein (LF_N-DHFR-L22R), which has 270 times lower affinity for MTX (*40*), translocation was not inhibited by MTX (Figure 7B). Liganding of the DTA moiety of LF_N-DTA also led to a blockage in translocation of this molecule. When 300 μM adenine (K_d for DTA = 30 μM) (*42*) was incubated with LF_NDTA during exposure to cells, translocation of the fusion protein was severely impaired (data not shown). Eighty micromolar NAD (K_d = 8 μM), a substrate of DTA, also blocked translocation, but less efficiently than adenine (*42*). These K_d values were measured at pH 8.2 and may not reflect the actual K_d values at pH 4.8.

As a complementary approach to demonstrating that unfolding is required for AT translocation, we used a fusion protein containing LF_N fused to the N-terminus of a mutant DTA containing an internal disulfide bond (LF_N-CC2). Proteins with internal disulfides generally migrate faster than their reduced counterparts in SDS−PAGE, and as seen in Figure 7C, the oxidized form of LF_N-CC2 migrated faster than the reduced form. A control mutant (LF_N-CS2) in which one cysteine was changed to serine displayed the same migration in the presence or absence of DTT (Figure 7C). When LF_N-CC2 (oxidized) was tested for translocation in the Pronase protection assay, no protected band was observed, but when DTT was added to the protein to reduce the disulfide bond prior to incubation with cells, a Pronase-protected band was observed (Figure 7D). A similar protected band was seen when the LF_N-CS2 construct was used (Figure 7D). Thus the disulfide bond in DTA blocked translocation of the fusion protein.

These results were corroborated by a functional assay. LF_NDTA had previously been shown to retain the catalytic properties of DTA and to inhibit protein synthesis in mammalian cells in a PA-dependent fashion (*24*). We compared the abilities of LF_NDTA, LF_NDTA-CC2, and LF_N-DTA-CS2 to inhibit protein synthesis as measured by the capability of treated cells to incorporate [^{3}H] leucine into newly synthesized proteins. As seen in Figure 7E, LF_NDTA-CC2 was at least 100-fold less toxic than either LF_NDTA or LF_NDTA-CS2. However, when the disulfide bond was reduced by the addition of DTT prior to incubation of the mutant protein with cells, the activity was restored to that of LF_NDTA.

Taken together, these data indicate that at least partial unfolding is necessary for the translocation of proteins via the AT pathway.

DISCUSSION

The crystallographic structure of the PA_{63} prepore (*23*) has given us for the first time the structure of a toxin B moiety complex that mediates pore formation and translocation. On the basis of this structure we have begun a quest to understand the mechanism of translocation by this toxin in detail. The main finding in the current work is that translocation of protein into cells by the AT pathway requires at least partial unfolding of the protein.

After binding to PA_{63} at the cell surface, radiolabeled ligands, including EF, LF, LF_N, and certain (but not all) LF_N-containing fusion proteins, were found to become resistant to Pronase E when the cells were exposed to acidic conditions. A brief low-pH incubation (30 s) was sufficient to induce this transition. Within the limits of the resolution of SDS−PAGE, the sizes of the protease-protected translocation products were unaltered from those of the original proteins, implying that the proteins traverse the membrane in intact form and become inaccessible to externally applied Pronase.

Although protection from Pronase degradation does not necessarily imply membrane traversal, the notion that protected proteins are released into the cytosol is supported

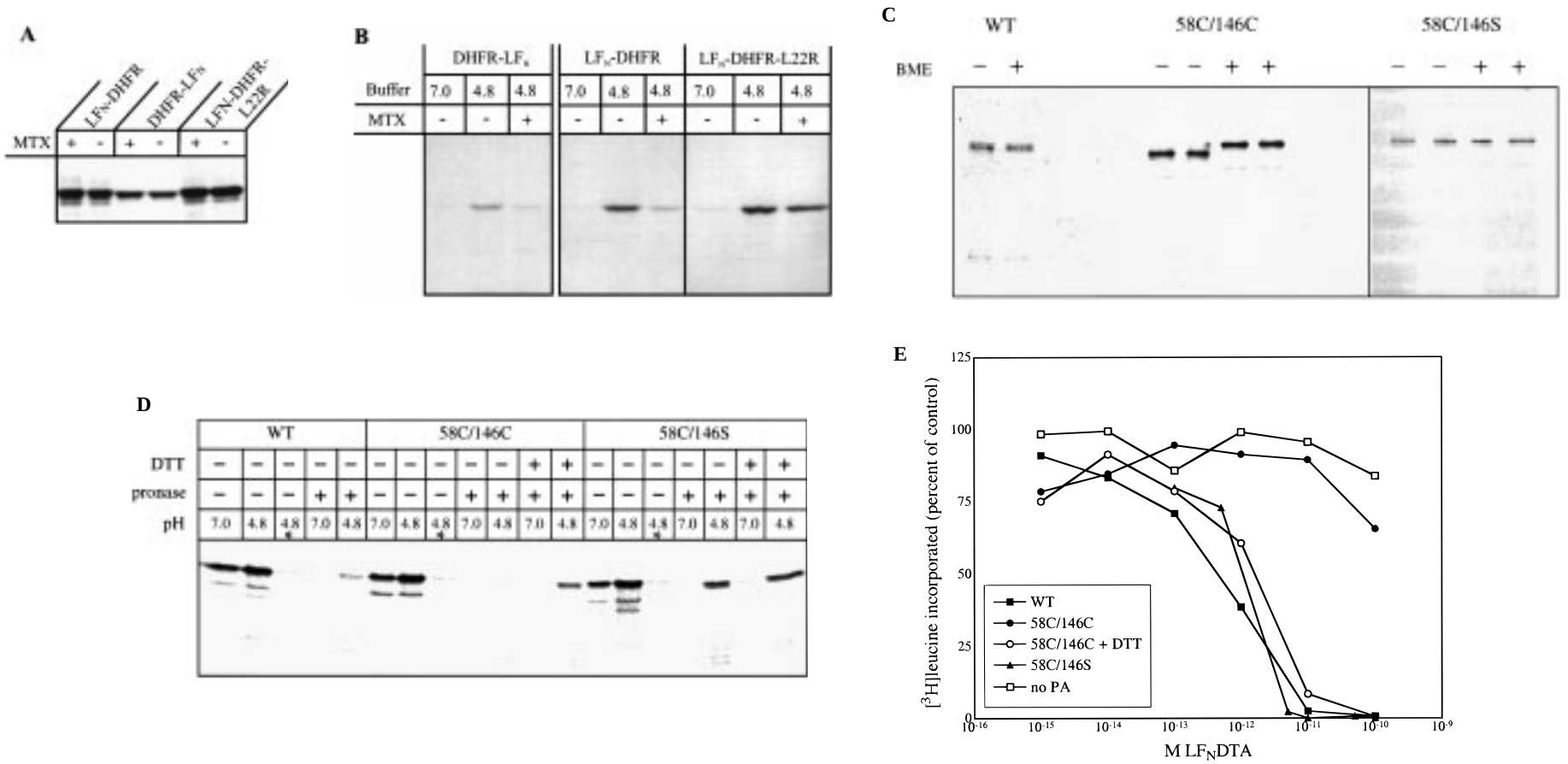

FIGURE 7: Translocation is inhibited by liganding or a novel disulfide bond. (A) Effect of MTX on binding of DHFR fusion proteins to cells. Nicked PA was bound to L6 cells for 2 h at 4 °C. Radiolabeled ligand was added with or without 55 μM MTX and incubated for 2 h at 4 °C. The cells were lysed and analyzed by SDS−PAGE and fluorography. (B) Effect of MTX on translocation of DHFR fusion proteins. The experiments were performed as in Figure 3A. nPA and radiolabeled DHFR fusion protein were bound to L6 cells. The cells were then exposed to neutral pH or to low pH in order to induce translocation of the fusion protein. Where indicated, 55 μM MTX was present during the binding of the radiolabeled DHFR fusion protein. The cells were treated with Pronase, lysed, and analyzed by SDS−PAGE and fluorography. (C) Differences in migration rates of WT and mutant LF_NDTAs on SDS−PAGE. Purified proteins were treated with Cu^{2+} phenanthroline and dialyzed extensively to remove reducing agents and phenanthroline. Reduced (+) and nonreduced (−) samples were compared. (D) Effects of an internal disulfide bond on translocation in the Pronase protection assay. CHO-K1 cells were treated with nPA at 4 °C for 2 h, followed by incubation with in vitro [^{35}S]methionine-labeled WT, LF_NDTA-CC2, or LF_NDTA-CS2 for 2 h at 4 °C. After washing, the cells were incubated with either pH 7.0 or 4.8 MES/gluconate buffer at 37 °C for 30 s. Cells were either lysed (− Pronase) or exposed to 2 mg/mL Pronase E (+ Pronase) in HEPES medium for 10 min at 37 °C. The cells detached by the Pronase treatment were transferred to microfuge tubes, washed with HEPES medium containing 1 mM PMSF at 4 °C, and lysed with 4 °C lysis buffer for 10 min. Samples were analyzed by SDS−PAGE and phosphorimagery. Lanes marked with an asterisk (*) indicate the absence of nPA to give an indication of nonspecific binding. (E) Cytotoxicity of mutant toxins. CHO-K1 cells were incubated overnight with increasing concentrations of WT (filled squares), artificially disulfide-bonded (58C/146C) (filled circles), or control (58C) LF_NDTA (filled triangles), and 2×10^{-8} M nPA. After washing, the cells were incubated with medium containing [^{3}H]leucine for 1 h at 37 °C. Total cellular protein was precipitated by 5% trichloroacetic acid. Precipitated material was solubilized in 100 mM KOH, and incorporated radioactivity was measured as a percentage of that in cells not receiving toxin treatment. Additionally, cells were treated with LF_N-CC2 reduced by DTT prior to incubation with cells (open circles), and with WT LF_NDTA in the absence of nPA (open squares). The data shown is the average of two trials.

by additional data. Expression of the enzymic activities of EF, DTA, and DHFR in vivo indicates that, at a minimum, the enzymic domains of these proteins fold correctly after translocation and are able to recognize their respective substrates within the cytosol. The fact that DTA fused to either the N-terminus or the C-terminus of LF_N inhibits protein synthesis in a PA-dependent manner implies that both the N-terminal and the C-terminal domains of translocated proteins become cytosolic and fold into an active form (*24*, *38*). Our data demonstrating that translocated LF_N is subject to the N-end rule-mediated protein degradation pathway in vivo also support the concept of cytosolic delivery. The inhibitory effects of lactacystin on LF_N degradation, together with the fact that LF_N was selectively degraded on the basis of the stabilizing ability of its N-terminal residue, imply degradation by the cytosolic proteasome (*36*).

Efficiencies of translocation estimated from the protease protection assay depended on both pH and temperature. The maximal rate of translocation observed at pH $\leq$ 5.2, measured with LF_N, is consistent with results reported earlier for the permeabilization of the plasma membrane to $^{86}Rb^+$ by nPA alone (*10*), suggesting that the insertion of the PA_{63} prepore represents the major determinant of pH dependence. A requirement of low pH for unfolding of the A moiety as an integral step in translocation is not excluded, however. We found little or no translocation when the low-pH pulse was conducted at 4 °C, although permeabilization to $^{86}Rb^+$ by nPA was seen at this temperature in earlier work (*10*, *43*). This discrepancy could reflect a temperature dependence of A-chain unfolding.

The efficiency of translocation of radiolabeled PA_{63} ligand under the chosen standard conditions (pH 4.8, 37 °C) ranged between 35% and 50% (with LF_N) and between 15% and 20% (with EF, LF, and LF_N fusion proteins). These values are similar to those observed in DT-mediated translocation across the plasma membrane (*44*, *45*). Although DTA and DHFR were translocated when fused to either the N-terminus or the C-terminus of LF_N, efficiency was somewhat greater with both proteins when the fusion was to the C-terminus of LF_N, yielding a domain order analagous to that in LF and EF. Whether size per se affects translocation efficiency remains to be determined, but it is clear that factors other than size are important determinants of efficiency. In contrast to the many heterologous proteins that are successfully translocated when fused to the C-terminus of LF_N (e.g., DTA, DHFR, CNTF (*24*, *37*, *38*, *46*)), we found several proteins that were apparently not translocated at all (acidic fibroblast growth factor, tetanus toxin light chain, basic fibroblast growth factor, HIV Tat protein, and botulinum toxin E light chain). The size range of proteins that are translocated (with LF_N and intact LF at low and high extremes, respectively) encompasses the set of those that are not. Translocation of an LF_N fusion of tetanus toxin light chain has been reported (*39*), but the construct employed in that study contains an additional domain from the heavy chain. The stoichiometry of ligand delivery is currently under study using this system.

Properties of proteins that determine their ability to be translocated by the LF_N/PA_{63} system remain to be determined. Evidence presented here supports the notion that translocation-competent proteins must undergo a transition to a partially or fully unfolded state. We found that introduction of an artificial disulfide bridge within the DTA moiety of LF_N-DTA, at a location that had been previously shown to block the translocation of DTA by the B chain of DT (*25*), effectively prevented PA-dependent translocation. This was demonstrated by both activity and protease protection assays. Reduction of the bridge permitted translocation. We also showed that translocation of LF_N-DHFR was blocked by the DHFR ligand MTX, whereas translocation of a similar fusion containing mutant DHFR (DHFR-L22R) with a drastically reduced affinity for MTX was unaffected by this ligand. Similarly, binding of adenine or NAD to the active site of DTA in LF_NDTA (*47*) blocked translocation of the fusion protein. Thus either of two methods of stabilizing the native conformation of a protein—introduction of an artificial disulfide bridge or liganding—caused a similar inhibitory effect. Similar findings have come from studies of translocation by DT (*25*, *41*).

As documented here and elsewhere, AT shows interesting similarities to DT in the functional aspects of translocation. In both toxins, the B moiety forms a pore in membranes (*12*, *17*), pore formation and translocation are pH-dependent processes and show similar pH dependence profiles (*12*, *18*, *48*), and there is a requirement for A-chain unfolding (*49*). In view of the dissimilar mechanisms of pore formation by AT and DT, these functional similarities apparently illustrate the convergence of two different evolutionary pathways to a function enabling a protein to insert into and translocate a second, bound protein across a membrane under acidic conditions. Although it is uncertain whether the enzymic moieties of these toxins traverse membranes via the aqueous pores formed by their respective B chains, this remains a viable model. It will be interesting to see how far the parallels in translocation between the two extend as the structures of the pores of the two toxins are understood in greater detail.

ACKNOWLEDGMENT

We are grateful to Jorunn Jacobsen for her expert technical assistance and to Lisa Ip and Anne Holck-Steen for the maintenance of the Olsnes cell cultures.

REFERENCES

1. Leppla, S. H. (1982) *Proc. Natl. Acad. Sci. U.S.A. 79*, 3162−6.
2. Mikesell, P., Ivins, B. E., Ristroph, J. D., and Dreier, T. M. (1983) *Infect. Immun. 39*, 371−376.
3. Leppla, S. H. (1995) in *Bacterial toxins and virulence factors in disease* (Moss, J., Iglewski, M., Vaughan, M., and Tu, A. T., Eds.) pp 543−572, Marcel Dekker, New York.
4. Leppla, S. H. (1984) *Adv. Cyclic Nucleotide Protein Phosphorylation Res. 17*, 189−98.
5. Klimpel, K. R., Arora, N., and Leppla, S. H. (1994) *Mol. Microbiol. 13*, 1093−1100.
6. Hammond, S. E., and Hanna, P. C. (1998) *Infect. Immun. 66*, 2374−2378.
7. Duesbery, N. S., Webb, C. P., Leppla, S. H., Gordon, V. M., Klimpel, K. R., Copeland, T. D., Ahn, N. G., Oskarsson, M. K., Fukasawa, K., Paull, K. D., and Vande Woude, G. F. (1998) *Science 280*, 734−737.
8. Hanna, P. C., Kruskal, B. A., Ezekowitz, R. A., Bloom, B. R., and Collier, R. J. (1994) *Mol. Med. (Tokyo) 1*, 7−18.
9. Klimpel, K. R., Molloy, S. S., Thomas, G., and Leppla, S. H. (1992) *Proc. Natl. Acad. Sci. U.S.A. 89*, 10277−81.
10. Milne, J. C., Furlong, D., Hanna, P. C., Wall, J. S., and Collier, R. J. (1994) *J. Biol. Chem. 269*, 20607−20612.

11. Gordon, V. M., Leppla, S. H., and Hewlett, E. L. (1988) *Infect. Immun. 56*, 1066−1069.
12. Blaustein, R. O., Koehler, T. M., Collier, R. J., and Finkelstein, A. (1989) *Proc. Natl. Acad. Sci. U.S.A. 86*, 2209−2213.
13. Koehler, T. M., and Collier, R. J. (1991) *Mol. Microbiol. 5*, 1501−1506.
14. Draper, R. K., and Simon, M. I. (1980) *J. Cell Biol. 87*, 849−854.
15. Sandvig, K., and Olsnes, S. (1980) *J. Cell Biol. 87*, 828−832.
16. London, E. (1992) *Biochim. Biophys. Acta 1113*, 25−51.
17. Kagan, B. L., Finkelstein, A., and Colombini, M. (1981) *Proc. Natl. Acad. Sci. U.S.A. 78*, 4950−4954.
18. Eriksen, S., Olsnes, S., Sandvig, K., and Sand, O. (1994) *EMBO J. 13*, 4433−4439.
19. Oh, K. J., Zhan, H., Cui, C., Hideg, K., Collier, R. J., and Hubbell, W. J. (1996) *Science 273*, 810−812.
20. Huynh, P. D., Cui, C., Zhan, H., Oh, K. J., Collier, R. J., and Finkelstein, A. (1997) *J. Gen. Physiol. 110*, 229−242.
21. Song, L., Hobaugh, M. R., Shustak, C., Cheley, S., Bayley, H., and Gouaux, J. E. (1996) *Science 274*, 1859−1866.
22. Benson, E. L., Huynh, P. D., Finkelstein, A., and Collier, R. J. (1998) *Biochemistry 37*, 3941−3948.
23. Petosa, C., Collier, R. J., Klimpel, K. R., Leppla, S. H., and Liddington, R. C. (1997) *Nature 385*, 833−8.
24. Milne, J. C., Blanke, S. R., Hanna, P. C., and Collier, R. J. (1995) *Mol. Microbiol. 15*, 661−666.
25. Falnes, P. O., Choe, S., Madshus, I. H., Wilson, B. A., and Olsnes, S. (1994) *J. Biol. Chem. 269*, 8402−8407.
26. Stenmark, H., Afansiev, B. N., Ariansen, S., and Olsnes, S. (1992) *Biochem. J. 281*, 619−625.
27. Laemmli, U. K. (1970) *Nature 227*, 680−685.
28. Falnes, P. Ø., and Olsnes, S. (1998) *EMBO J. 17*, 615−625.
29. Reiss, Y., Kaim, D., and Hershko, A. (1988) *J. Biol. Chem. 263*, 2693−2698.
30. Blanke, S. R., Huang, K., Wilson, B., Papini, E., Covacci, A., and Collier, R. J. (1994) *Biochemistry 33*, 5155−5161.
31. Zhan, H., Choe, S., Huynh, P. D., Finkelstein, A., Eisenberg, D., and Collier, R. J. (1994) *Biochemistry 33*, 11254−11263.
32. Milne, J. C., and Collier, R. J. (1993) *Mol. Microbiol. 10*, 647−653.
33. Varshavsky, A. (1997) *Genes Cells 2*, 13−28.
34. Gonda, D. K., Bachmair, A., Wunning, I., Tobias, J. W., Lane, W. S., and Varshavsky, A. (1989) *J. Biol. Chem. 264*, 16700−16712.
35. Hopp, T. P., Prickett, K. S., Price, V. L., Libby, R. T., March, C., Cernti, D. P., Urdal, D. L., and Conlon, P. J. (1988) *Bio/Technology 6*, 1204−1210.
36. Lee, D. H., and Goldberg, A. L. (1996) *J. Biol. Chem. 271*, 27280−27284.
37. Arora, N., Klimpel, K. R., Singh, Y., and Leppla, S. H. (1992) *J. Biol. Chem. 267*, 15542−15548.
38. Arora, N., and Leppla, S. H. (1994) *Infect. Immun. 62*, 4955−61.
39. Arora, N., Williamson, L. C., Leppla, S. H., and Halpern, J. L. (1994) *J. Biol. Chem. 269*, 26165−71.
40. Ercikan-Abali, E. A., Waltham, M. C., Dicker, A. P., Schweitzer, B. I., Gritsman, H., Banerjee, D., and Bertino, J. R. (1996) *Mol. Pharmacol. 49*, 430−437.
41. Klingenberg, O., and Olsnes, S. (1996) *Biochem. J. 313* (Pt. 2), 647−653.
42. Kandel, J., Collier, R. J., and Chung, D. W. (1974) *J. Biol. Chem. 249*, 2088−2097.
43. Zhao, J., Milne, J. C., and Collier, R. J. (1995) *J. Biol. Chem. 270*, 18626−18630.
44. Moskaug, J. Ø., Sandvig, K., and Olsnes, S. (1988) *J. Biol. Chem. 263*, 2518−2525.
45. Falnes, P. Ø., Wiedlocha, A., Rapak, A., and Olsnes, S. (1995) *Biochemistry 34*, 11152−11159.
46. Arora, N., and Leppla, S. H. (1993) *J. Biol. Chem. 268*, 3334−3341.
47. Chung, D., and Collier, R. J. (1977) *Biochim. Biophys. Acta 483*, 248−257.
48. Brasseur, R., Cabiaux, V., Falmagne, P., and Ruysschaert, J. M. (1986) *Biochem. Biophys. Res. Commun. 136*, 160−168.
49. Tortorella, D., Sesardic, D., Dawes, C. S., and London, E. (1995) *J. Biol. Chem. 270*, 27439−27445.

BI981436I